the plant journal

SEB Society for Experimental Biology

The Plant Journal (2014) **78,** 646–658 doi: 10.1111/tpj.12501

Decreased capacity for sodium export out of Arabidopsis chloroplasts impairs salt tolerance, photosynthesis and plant performance

Maria Müller[1], Hans-Henning Kunz[2], Julian I. Schroeder[2], Grant Kemp[3], Howard S. Young[3] and H. Ekkehard Neuhaus[1,*]

[1]*Plant Physiology, University of Kaiserslautern, Erwin Schrödinger Straße, Kaiserslautern D–67653, Germany,*

[2]*Division of Biological Sciences, Cell and Developmental Biology Section & Center for Food and Fuel for the 21st Century, University of California at San Diego, 9500 Gilman Drive, 0116 La Jolla, CA 92093–0116, USA, and*

[3]*Department of Biochemistry, University of Alberta, Edmonton, AB T6G 2H7, Canada*

Received 27 November 2013; revised 5 February 2014; accepted 26 February 2014; published online 11 March 2014.

*For correspondence (email neuhaus@rhrk.uni-kl.de).

SUMMARY

Salt stress is a widespread phenomenon, limiting plant performance in large areas around the world. Although various types of plant sodium/proton antiporters have been characterized, the physiological function of NHD1 from *Arabidopsis thaliana* has not been elucidated in detail so far. Here we report that the NHD1–GFP fusion protein localizes to the chloroplast envelope. Heterologous expression of *AtNHD1* was sufficient to complement a salt-sensitive *Escherichia coli* mutant lacking its endogenous sodium/proton exchangers. Transport competence of NHD1 was confirmed using recombinant, highly purified carrier protein reconstituted into proteoliposomes, proving Na^+/H^+ antiport. *In planta NHD1* expression was found to be highest in mature and senescent leaves but was not induced by sodium chloride application. When compared to wild-type controls, *nhd1* T–DNA insertion mutants showed decreased biomasses and lower chlorophyll levels after sodium feeding. Interestingly, if grown on sand and supplemented with high sodium chloride, *nhd1* mutants exhibited leaf tissue Na^+ levels similar to those of wild-type plants, but the Na^+ content of chloroplasts increased significantly. These high sodium levels in mutant chloroplasts resulted in markedly impaired photosynthetic performance as revealed by a lower quantum yield of photosystem II and increased non-photochemical quenching. Moreover, high Na^+ levels might hamper activity of the plastidic bile acid/sodium symporter family protein 2 (BASS2). The resulting pyruvate deficiency might cause the observed decreased phenylalanine levels in the *nhd1* mutants due to lack of precursors.

Keywords: sodium, plastid, salt tolerance, transport, membrane protein, Arabidopsis.

INTRODUCTION

The presence of high salt-containing soils at coastal regions is not surprising, but increased salinity in fact represents a global problem that is derived from improper agricultural use (Munns, 2005). Twenty per cent of irrigated agronomically used land suffers from high salt concentrations (Munns, 2005), making sodium a potential toxic solute which severely limits crop productivity (Bartels and Sunkar, 2005). In contrast, 'halophytes', organisms that naturally live on soils with high NaCl levels, are able to complete their life cycle at soil sodium concentrations exceeding 200 mM.

A major mechanism of sodium toxicity in plants is thought to be based on competition of Na^+ with K^+ at binding sites of enzymes that require potassium as a co-factor for full activity (Flowers and Dalmond, 1992). In addition, high external sodium chloride concentrations provoke imbalances of the overall cellular solute homeostasis, further impairing most physiological processes and also affecting the control of gene expression (Zhu, 2002). To cope with high sodium chloride levels, plants have developed various strategies, comprising avoidance of Na^+ entry into the plant body or increased tolerance of high Na^+ levels in various organs (Flowers and Colmer, 2008). The latter strategy is often achieved by intracellular sequestration of sodium into the large cell vacuole (Martinoia *et al.*, 2007), control of Na^+ accumulation in plant leaves (Mäser *et al.*, 2002; Horie *et al.*, 2009), or Na^+ export across the plasma membrane (Blumwald, 2000).

In mammalian cells, specific carriers, named NHE, export protons in exchange with sodium and this catalytic activity

contributes to the regulation of cytoplasmic pH. (Brett *et al.*, 2005). In marked contrast, in bacteria, yeast and plants, plasma membrane located antiporters mediate sodium export in exchange with protons and these carriers are essential for the removal of cytosolic sodium (Chen and Fliegel, 2008). In plant cells, proton-motive forces not only dictate sodium export across the plasma membrane, but also intracellular sodium compartmentation into the acidic vacuole (Martinoia *et al.*, 2007).

Similar to animal and yeast systems, plant genomes encode various sodium hydrogen exchangers (NHX) isoforms, e.g. Arabidopsis harbors six isoforms (Brett *et al.*, 2005). Over-expression of the vacuolar-located NHX1 in tomato (*Solanum lycopersicum*) and several other species conferred increased salt tolerance (Apse *et al.*, 1999; Zhang and Blumwald, 2001; Zhang *et al.*, 2001; Ohta *et al.*, 2002; Xue *et al.*, 2004; Yin *et al.*, 2004), underpinning the importance of subcellular Na^+ sequestration. However, recent data have indicated similar affinities of NHX1 and NHX2 for both Na^+ and K^+ (Barragan *et al.*, 2012). Some NHX isoforms from Arabidopsis locate to other endomembranes than vacuoles, such as the endoplasmic reticulum or Golgi-derived structures (endosomes), and are critical for vesicle trafficking and concomitant salt tolerance (Bassil *et al.*, 2011).

Sodium hydrogen antiporter (NHAD)-type carriers exist in all vascular and non-vascular plants, including mosses and algae (Barrero-Gil *et al.*, 2007). NHAD from the salt-tolerant ice plant *Mesembryanthemum crystalllinum* (McNHAD) locates to the chloroplast envelope, and heterologous expression of McNHAD complements the *Escherichia coli NhaA NhaB* mutant, which lacks endogenous Na^+/H^+ antiporters (Cosentino *et al.*, 2010). Two isoforms of NHAD carriers, NHD1 and NHD2, exist in Arabidopsis (Schwacke *et al.*, 2003). The physiological importance of these carrier proteins is unknown, although Arabidopsis chloroplasts possess at least two further Na^+-dependent transport systems; the thylakoid-located Na^+/Pi symporter anion transporter 1 (Pavon *et al.*, 2008), and the envelope-located sodium-dependent pyruvate transporter bile acid/sodium symporter family protein 2 (BASS2; Furumoto *et al.*, 2011). As the *Mesembryanthemum* homolog of NHD1 localizes to the plastid envelope, and co-expression of *BASS2* and *NHD1* in *E. coli* stimulates BASS2 activity, it has been proposed that the NHD1 protein may contribute to the export of stromal sodium derived from previous Na^+/pyruvate co-import via BASS2 (Furumoto *et al.*, 2011).

However, so far it has not been demonstrated that NHD1 from Arabidopsis is localized at the chloroplastic envelope, nor has the exact biochemical mechanism of NHD1 or its effect on plastid Na^+ levels or on plant performance in the presence of salt been demonstrated. Therefore, we address the following questions:

(1) Does NHD1 transport sodium and what is its subcellular localization in Arabidopsis?
(2) How does the *NHD1* gene respond to rising NaCl levels?
(3) Does Arabidopsis, a model glycophyte, accumulate sodium in the chloroplast as a consequence of salt treatment, as seen in halophytes?
(4) What are the physiological consequences of decreased sodium export out of Arabidopsis chloroplasts?

RESULTS

NHD1–GFP localizes to the plastid envelope

So far, chloroplast envelope localization of NHD1 has only been assumed (Furumoto *et al.*, 2011). AtNHD1 and its homolog from *M. crystallinum* (McNHAD) share 86% similarity at the amino acid sequence level (Figure S1), and the plastidic location of the latter has been demonstrated by use of a GFP fusion (Cosentino *et al.*, 2010). However, a proteomic study identified NHD1 in enriched Arabidopsis plasma membranes (Mitra *et al.*, 2009), resulting in a need to obtain experimental data on the subcellular localization of AtNHD1.

By expression of the *NHD1::GFP* mRNA construct in mesophyll protoplasts, we were able to demonstrate the subcellular location of the corresponding fusion protein. After transformation of isolated Arabidopsis mesophyll protoplasts with the *NHD1::GFP* mRNA, the GFP signal co-localizes with the red chlorophyll auto-fluorescence, confirming a plastidic localization (Figure 1a–c). The plastidial localization was confirmed in a second system by transient expression of *NHD1::GFP* in tobacco protoplasts (Figure 1d–f). To further confirm the envelope localization of NHD1, we co-transformed tobacco protoplasts with *NHD1::GFP* and *TAP38::RFP* mRNA, encoding a thylakoid-associated protein phosphatase (Pribil *et al.*, 2010). These proteins do not show any significant co-localization (Figure S2a–c), and the corresponding scatter plot revealed a co-localization rate of only 6.8% (Figure S2d). Thus, localization of NHD1 to the thylakoid may be excluded.

NHD1 catalyzes sodium/proton antiport

The sodium transport activity of the NHAD homologs from *M. crystallinum* and *Populus euphratica* (poplar) has been demonstrated by complementation of *E. coli* knockout strains lacking endogenous Na^+/H^+ antiporters (Cosentino *et al.*, 2010). The *E. coli* strain *KNabc* (Δ*nha*A, Δ*nha*B Δ*cha*A; Nozaki *et al.*, 1996) was transformed with a plasmid harboring *AtNHD1* under the control of the isopropyl-β–D–thiogalactopyranoside-inducible TAC promoter, and cell growth rates were quantified in the presence of sodium (Figure 2a; control cells carried the empty control plasmid pTAC–MAT–Tag1). Heterologous expression of *NHD1* increased the sodium tolerance of transformed *KNabc* cells

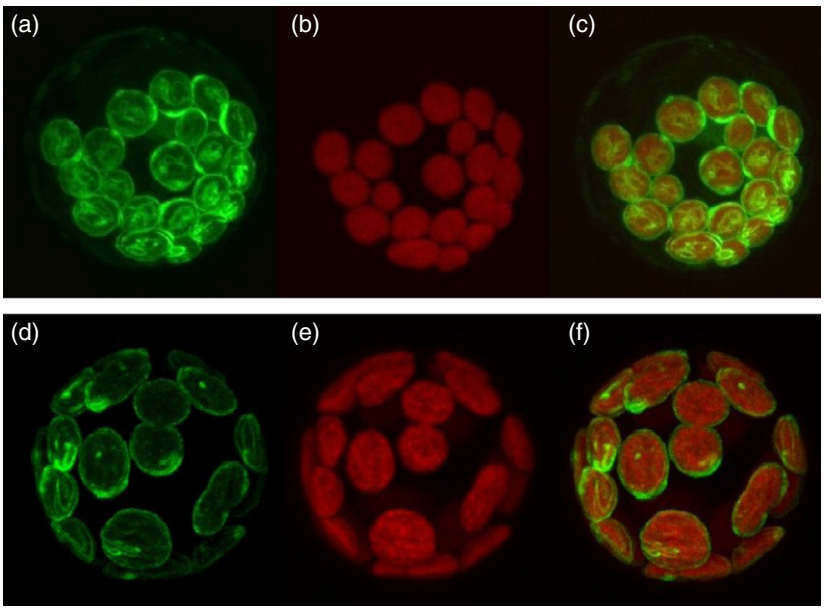

Figure 1. Subcellular localization of the NHD1–GFP-fusion protein construct in Arabidopsis (a–c) and tobacco (d–f) protoplasts.
Images show GFP fluorescence (a,d), chlorophyll autofluorescence (b,e) and merged images of GFP and chlorophyll autofluorescence (c,f).

significantly when compared to control cells, suggesting Na^+ transport competence of NHD1 (Figure 2a). To elucidate the sodium response of NHD1-expressing *E. coli* mutants in more detail, we quantified the growth over the entire 15 h of cultivation (Figure S3). The presence of 200 mM NaCl leads to substantial growth inhibition of the *E. coli KNabc* strain (Figure S3a), but the expression of *NHD1* resulted in a less pronounced growth defect (Figure S3b). Increased sodium tolerance due to *NHD1*-expression becomes particularly visible by monitoring growth of salt-treated and salt-untreated bacteria over time. To allow better comparison, maximal growth of *KNabc* bacteria and of *NHD1*-expressing cells was set to 100% (control), respectively and time dependent growth (either in presence or absence of salt) was calculated according to the corresponding controls (Figure S3c). To obtain further independent evidence that NHD1 acts as a sodium carrier, we quantified sodium levels in *KNabc* cells and *NHD1*-expressing cells grown in the absence or presence of 200 mM NaCl (Figure 2b). In the absence of NaCl, the internal sodium levels of both cell types were indistinguishable, but in the presence of NaCl, expression of *NHD1* led to significantly decreased levels of cellular sodium after 7 or 14 h growth compared to *KNabc* cells (Figure 2b).

The *E. coli* system does not allow us to analyze whether NHD1 directly mediates sodium/proton antiport. To overcome this limitation, we developed a protocol allowing both biochemical purification of recombinant AtNHD1 synthesized in *E. coli* and subsequent functional reconstitution in proteoliposomes. We showed here that expression of *NHD1* in *E. coli* leads to functional insertion of the recombinant carrier in the bacterial plasma membrane (Figure 3a,b, lane 1), and that use of immobilized metal-ion affinity chromatography (IMAC) allowed enrichment of the decahistidine-tagged NHD1 protein to high purity (Figure 3a, lane 2). The His-tagged NHD1 protein had an apparent molecular mass of approximately 57 kDa (Figure 3a,b, lane 2).

Purified His-tagged NHD1, or the rabbit sarcoplasmic reticulum-located Ca^{2+} ATPase SERCA as a control, were reconstituted into artificial liposomes. A pH gradient across the proteoliposomal membrane was created via dilution into ammonium-free buffer medium, resulting in acid loading (Venema *et al.*, 2002; Moncoq *et al.*, 2008). In the absence of external sodium chloride, NHD1-containing proteoliposomes did not export protons, as indicated by the unchanged pyranine fluorescence within the first 100 sec of the experiment (Figure 3c). However, after addition of 200 mM NaCl, NHD1-harboring proteoliposomes exhibited sodium import coupled to proton antiport at high rates. The concomitant increase of pyranine fluorescence reached saturation after approximately 200 sec (Figure 3c). In marked contrast, control proteoliposomes reconstituted with SERCA protein did not show detectable proton export upon sodium application (Figure 3c), confirming the specificity of NHD1-mediated Na^+/H^+ exchange. The specificity of NHD1-mediated sodium/proton antiport is also underlined by two further observations: first, the relative pyranine fluorescence change is dependent on the NHD1 protein concentration reconstituted in liposomes (Figure 3c), and second, addition of KCl does not induce a significant pyranine fluorescence (Figure 3d). To obtain further evidence that the NHD1 transport observed in intact *E. coli* cells (Figure 2 and Figure S3) is due to sodium/proton antiport, we measured NaCl-induced pH changes in corresponding bacterial cells (Figure 3e). In the absence of additional NaCl, the external medium pH of control cells

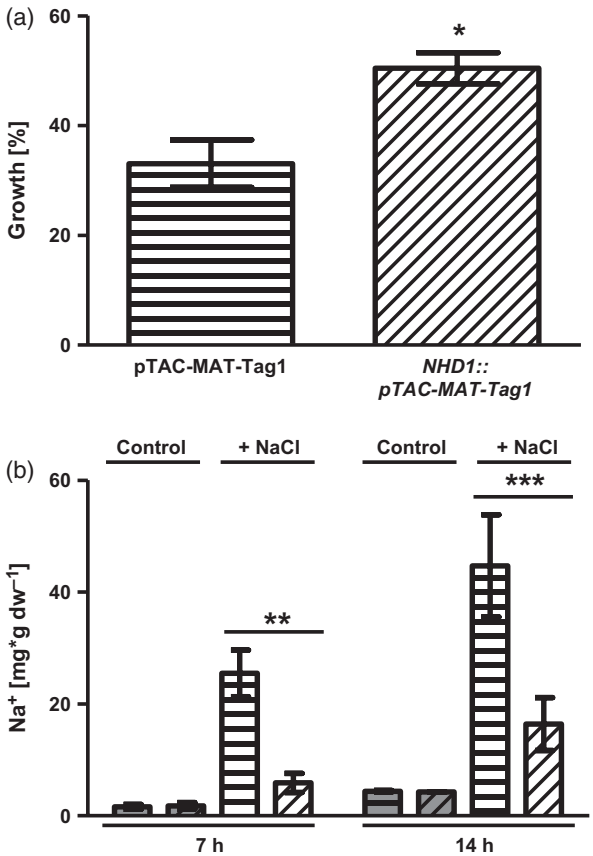

Figure 2. Functional complementation of the *E. coli* knockout strain *KNabc* by recombinant NHD1 protein synthesis.
(a) Growth was observed at OD_{600} until a steady state was reached. The growth rate is shown as a percentage of the maximum growth of *KNabc* cells treated with 200 mM KCl. Values are means ± SE of three individual experiments, each with three technical replicates. The asterisk indicates a statistically significant difference compared with the control (pTAC–MAT–Tag1) (*$P < 0.05$, Student's *t* test).
(b) Na^+ content was measured in *Knabc* cells carrying the empty pTAC-MAT-Tag1 vector (horizontal striped bars) or NHD1 (diagonal striped bars) after 7 and 14 h of growth. Cells were grown in LBK medium, pH 7.5, supplemented with 200 mM KCl (gray bars) or 200 mM NaCl (white bars). Values are means ± SE of seven individual experiments. Asterisks indicate statistically significant differences (**$P < 0.01$, ***$P < 0.001$, two-way ANOVA).

and cells expressing NHD1 was similar (approximately 7.2, Figure 3e). In contrast, addition of NaCl resulted in a significantly higher pH value in the medium containing *NHD1*-expressing cells, compared with control cells (Figure 3e). This indicates that sodium that entered the *E. coli* cells non-specifically is re-exported by NHD1.

The *NHD1* gene exhibits a tissue-specific expression pattern but is not salt-induced

To obtain insights into the tissue specificity of *NHD1* gene expression, quantitative RT–PCR analyses were performed (Figure 4a). *NHD1* mRNA levels were comparably low in seeds, roots, shoots, flowers and developing siliques (Figure 4a). In contrast, *NHD1* expression in the leaf tissues was dependent on the developmental stage. While young leaves contained only fairly low levels of *NHD1* mRNA, mature leaves accumulated approximately fivefold higher levels, which remained constant throughout leaf senescence (Figure 4a).

Higher plants possess several carrier proteins that are able to transport sodium against the electrochemical gradient. In addition to NHD1, NHX1 (an intracellular $Na^+(K^+)/H^+$ antiporter) contributes to Na^+ tolerance (Hernandez *et al.*, 2009; Barragan *et al.*, 2012; Bassil *et al.,* 2011), and was shown to be induced by NaCl treatment (Yokoi *et al.*, 2002). This prompted us to compare the expression pattern of both *NHD1* and *NHX1* in response to sodium chloride. Therefore, Arabidopsis plants were grown for 4 weeks on sand, and then exposed to 150 mM NaCl for 8 days (Figure 4b). The levels of the mRNA encoding the vacuolar Na^+/H^+ exchanger NHX1 remained constant for the first 4 days of sodium treatment, and increased 2.3-fold over the next 4 days (Figure 4b). In contrast, *NHD1* levels did not change within the first 4 days of salt stress but decreased approximately 30% compared to the control after 8 days of salt treatment (Figure 4b).

Isolation of *nhd1* mutant plants

Among the available Arabidopsis *nhd1* T–DNA insertion lines, only one homozygous knockout line (Salk008491, *nhd1–1*) was identified. The fact that *nhd1–1* mutants are viable but only heterozygous *nhd1–2* mutants (Sail107_F07) were detected suggests the existence of a second and lethal T–DNA insertion in *nhd1–2* plants. To obtain a second *nhd1* line, homozygous *nhd1–1* mutants were crossed with heterozygous *nhd1–2* mutants (Figure S4). As backcrossing to *nhd1–1* seeds takes place among these mutants, every generation must be screened for *nhd1–1* × *nhd1–2* plants by PCR or BASTA selection.

As a result, *nhd1–1* × *nhd1–2* mutants are still genetically related to the *nhd1–1* mutants. To obtain a further control, *nhd1–1* plants were complemented with endogenous Arabidopsis *NHD1* cDNA driven by the *Ubiquitin10* promoter (Krebs *et al.*, 2012) and fused to VENUS at the 3′-end to verify plastidic localization *in planta* (Figure S4). After screening independent *nhd1–1::UBQ10:NHD1* mutants, three independent lines (numbers 28, 31 and 34) were isolated that exhibited 9-, 11- and 6-fold increased *NHD1* mRNA levels compared to wild-type (Wt) (Figure S4).

nhd1–1::UBQ10:NHD1 mutants were used to determine plastidic sodium concentration, photosynthetic performance and amino acid levels upon salt stress (see below). As none of the results revealed significant differences between Wt and *nhd1–1::UBQ10:NHD1* mutants, we conclude that *nhd1–1* mutants are rescued by over-expression of a plastidic Na^+/H^+ antiporter (Figures 5–8 and Figure S4h).

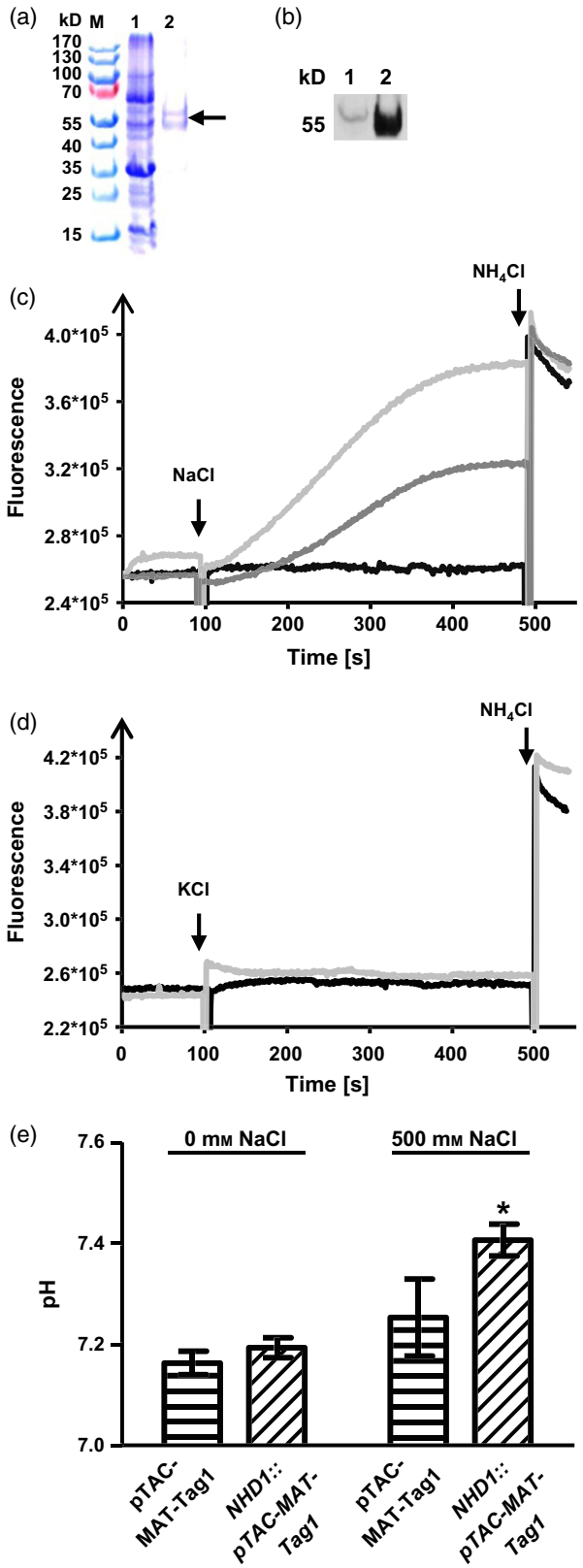

Figure 3. Transport activity of NHD1.
(a,b) SDS–PAGE (a) and Western blot (b) of IMAC purification of recombinant synthesized NHD1. Lane M, molecular mass markers. Lane 1, 25 μg total membrane proteins from NHD1-synthesizing *E. coli* cells. Lane 2, 1 μg purified NHD1.
(c,d) Either 2.8 μg (light grey), 1.4 μg NHD1 (dark grey) NHD1 or as a control 2.8 μg SERCA (black) were reconstituted into proteoliposomes. Na^+/H^+ (c) or K^+/H^+ (d) exchange was started by addition of NaCl or KCl. The experiment was stopped by addition of NH_4Cl. Transport activity was observed by an increase in pyranine fluorescence. The results of representative transport and control experiments are shown.
(e) *E. coli KNabc* cells either expressing *NHD1* or carrying the empty pTAC-MAT-Tag1 vector were supplemented with 0 or 500 mM NaCl. After pelleting the cells, the pH was measured in the supernatant. Values means ± SE of 14 individual experiments. The asterisk indicates a statistically significant difference compared with the control (pTAC–MAT–Tag1) ($P < 0.05$, Student's *t* test).

nhd1 knockout mutants are significantly less tolerant to sodium than wild-type plants

Chloroplasts from the halophytes *M. crystallinum* and *Suaeda maritima* accumulate high concentrations of sodium under salt stress conditions (Harvey *et al.*, 1981; Cosentino *et al.*, 2010). In this study, we analyzed whether the glycophytic model plant Arabidopsis is able to accumulate sodium to similar high levels in its chloroplasts.

When grown in liquid culture, wild-type, *nhd1–1* and all three *nhd1–1::UBQ10:NHD1* lines developed at almost the same efficiency, reaching approximately 1600–1800 mg biomass within 10 days (Figure 5a). Exogenous 100 mM NaCl application led to a decrease of approximately 40% in the fresh weight in wild-type controls and *nhd1–1::UBQ10:NHD1* plants to 900–1200 mg fresh biomass (Figure 5b). However, under the same conditions, growth of *nhd1–1* mutants was even more inhibited compared to Wt plants, producing 400 mg fresh biomass (Figure 5b). Similarly, the total chlorophyll content was comparable in all mutant lines and wild-type under control conditions (Figure 5c), but was significantly reduced in the *nhd1–1* mutant compared to Wt after salt treatment. As seen for the fresh weight biomass (Figure 5b), *nhd1–1* showed a strongly decrease chlorophyll content of approximately 88% compared to Wt plants after salt exposure (Figure 5d). *nhd1–1::UBQ10:NHD1* plants showed no significant differences in fresh weight and chlorophyll content upon salt treatment compared to Wt (Figure 5b,d).

When grown in liquid half-strength MS medium, all plants lines had similar biomass and morphology (Figure 5e). The additional presence of 100 mM NaCl in the medium after 7 days inhibited growth of all plant lines. However, *nhd1–1* plants exhibited stronger growth retardation compared to Wt and *nhd1–1::UBQ10:NHD1* plants (Figure 5b,d). *nhd1–1* individuals hardly developed at all after

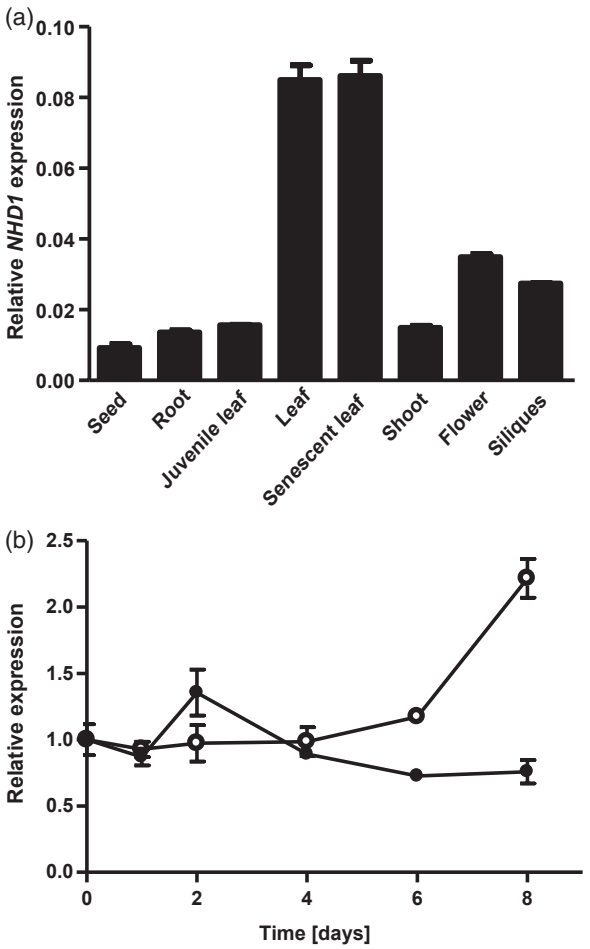

Figure 4. Relative expression levels of *NHD1* and *NHX1*, revealed by quantitative RT–PCR.
(a) Relative transcript level of *NHD1* in various Arabidopsis tissues. Data are normalized to the housekeeping gene *EF-1α*.
(b) Relative transcript levels of *NHD1* (closed circles) and *NHX1* (open circles) in Arabidopsis plants, grown on sand for 4 weeks and watered for 8 days with half-strength MS medium containing 150 mM NaCl. Samples were taken after 0, 2, 4, 6 and 8 days. Data are normalized to the onset of NaCl application.
Data represent means ± SE of three independent biological replicates.

salt application, and contained only minor amounts of chlorophyll (Figure 5e).

nhd1 mutants show altered intracellular sodium compartmentation

To investigate whether Wt and *nhd1* mutant plants are able to accumulate excess sodium within chloroplasts, we grew plants on sand supplemented with 150 mM NaCl for 3 days under short-day conditions prior to analysis of chlorophyll levels, total Na^+ contents in leaf tissue and plastidic sodium levels. As described above, all three *nhd1–1::UBQ10:NHD1* lines exhibited similar reactions upon salt treatment. Therefore, we focused these analyses on *nhd1–1::UBQ10:NHD1* line 31, *nhd1–1* and *nhd1–1* × *nhd1–2* mutants (Figure 6a–c).

Application of 150 mM NaCl for only 3 days prior to analyses did not have specific effects on total chlorophyll levels in Wt and mutants, as all plant lines contained approximately 1–1.5 mg Chl $(g\ FW)^{-1}$ (Figure 6a). Both Wt and mutant plants accumulated up to 680 μg Na^+ $(g\ FW)^{-1}$ after watering with 150 mM NaCl (Figure 6b, right), which is approximately 15 times more sodium compared to non-treated control plants (Figure 6b, left).

Interestingly, the additional presence of NaCl in the daily applied water led to a doubled Na^+ content in isolated Wt and *nhd1–1::UBQ10:NHD1* chloroplasts (Figure 6c). Chloroplasts isolated from salt-treated *nhd1* knockout mutants accumulated even higher sodium amounts, reaching 4.1 μg Na^+ (μg Chl)$^{-1}$ in *nhd1–1* and 3.5 μg Na^+ (μg Chl)$^{-1}$ in *nhd1–1* × *nhd1–2* mutants, respectively (Figure 6c, right). This three- to fourfold increase represents a significant increase in plastidic sodium concentration compared to chloroplasts isolated from Wt and *nhd1–1::UBQ10:NHD1* plants.

nhd1 knockout mutants are impaired in photosynthetic reactions upon salt stress

As indicated by GFP and VENUS fusions, NHD1 localizes to the chloroplast envelope (Figure 1a–f and Figure S4h). In line with this, loss of the protein led to increased plastidial Na^+ concentration upon salt treatment (Figure 6c), accompanied by a significantly reduced chlorophyll content and paler leaves (Figure 4). Therefore, we were interested in monitoring the effects of loss of NHD1 on chloroplast-localized photosynthetic reactions.

By use of the pulse-amplitude modulated fluorescence analysis, it is possible to quantify both the quantum efficiency of photosystem II (ΦPSII) and the degree of non-photochemical quenching (NPQ). ΦPSII is a direct measure of the relative use of light energy for photosynthesis, whereas the NPQ provides insight into the degree of quenching of excess light that cannot be used for photosynthesis (Maxwell and Johnson, 2000). In the case of Wt and *nhd1–1::UBQ10:NHD1* plants, the absence or presence of 150 mM NaCl for 3 days did not alter ΦPSII (approximately 0.43) (Figure 7a). In contrast, NaCl treatment of *nhd1* knockout plants significantly reduced ΦPSII by up to 15% compared to untreated control plants (Figure 7a).

Similarly, the NPQ of Wt and *nhd1–1::UBQ10:NHD1* plants was not altered by the presence of 150 mM NaCl for 3 days (Figure 7b). In contrast, *nhd1–1* and *nhd1–1* × *nhd1–2* mutants showed a significant increase in NPQ of 12% compared to control conditions.

nhd1 knockout mutants exhibit altered levels of phenylalanine and tyrosine

Recently, NHD1 activity in the C4 species *Flaveria bidentis* has been shown to be associated with the chloroplastic

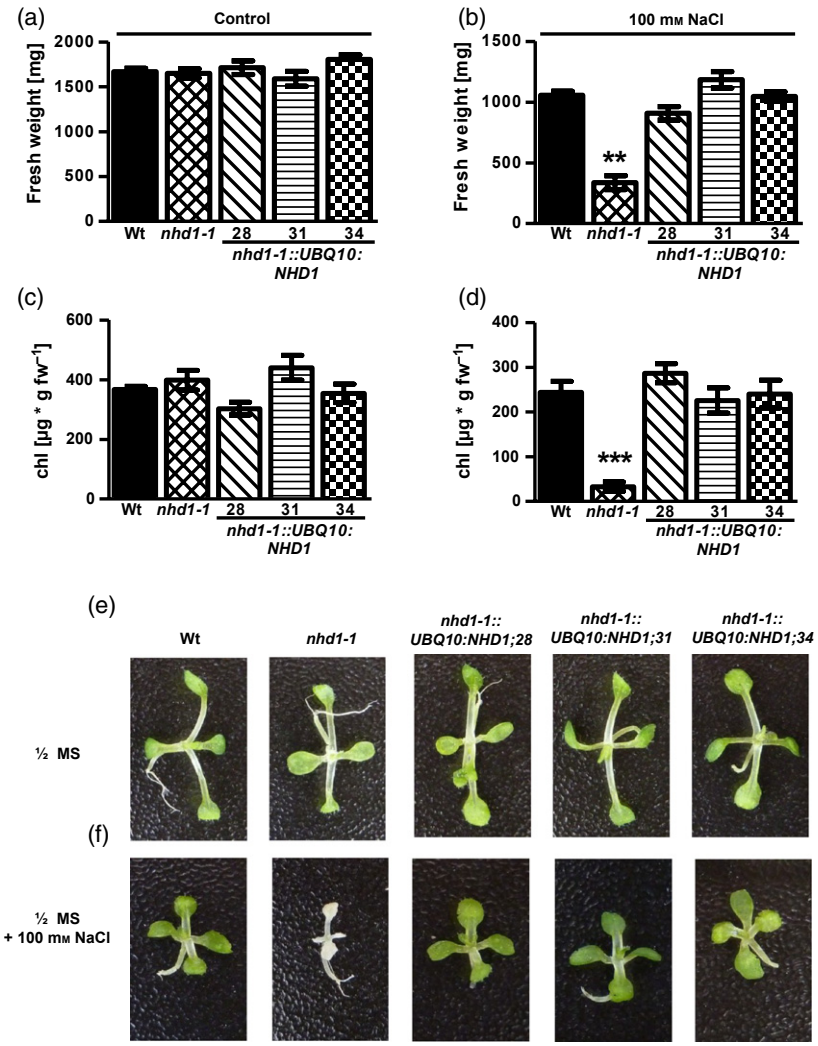

Figure 5. Analysis of Arabidopsis seedlings grown with or without 100 mM NaCl in liquid culture.
Wt, *nhd1–1* and *nhd1–1::UBQ10:NHD1* plants were grown in liquid culture in half-strength MS medium. After 7 days, the medium was replaced with fresh medium with or without 100 mM NaCl. Plants were harvested 96 h after the change of medium.
(a–d) Fresh weight (a,b) and chlorophyll content (c,d) were determined. Values are means ± SE of three biological replicates, each with at least two technical replicates. Asterisks indicate statistically significant differences compared with Wt (**$P < 0.01$, ***$P < 0.001$, two-way ANOVA).
(e,f) Representative 11-day-old Wt, *nhd1–1* and *nhd1–1::UBQ10:NHD1* seedlings, for which medium was changed 96 h prior to imaging.

Na^+-driven pyruvate carrier BASS2. Pyruvate uptake into plastids is required to fuel biosynthesis of aromatic amino acids. To investigate whether altered NHD1 activity is involved in with synthesis of aromatic amino acids, we quantified the leaf content of 17 biogenic amino acids in Wt plants, *nhd1* knockout and *nhd1–1::UBQ10:NHD1* mutants under control and salt stress conditions (Table S1). With the exceptions of phenylalanine and tyrosine, none of the measured 17 biogenic amino acids showed a different pattern in *nhd1* mutants compared to corresponding Wt plants (Table S1). Interestingly, when compared to Wt and *nhd1–1::UBQ10:NHD1* plants, the levels of phenylalanine were significantly decreased in all genotypes but only if plants were treated with 150 mM NaCl (Figure 8a). Wt and *nhd1–1::UBQ10:NHD1* plants contained 30 nmol g FW^{-1} phenylalanine under salt stress, whereas *nhd1* knockout mutants contained only between 24 and 26 nmol g FW^{-1} (Figure 8a). Tyrosine levels increased approximately 60% in *nhd1* knockout mutants upon salt stress, but there was no alteration in tyrosine levels in Wt and *nhd1–1::UBQ10:NHD1* plants.

DISCUSSION

Excess sodium impairs biochemical processes and metabolism in all cell types. To prevent these unfavorable situations, sodium/proton exchangers are present in organisms at all evolutionary levels. Plant NHAD1 proteins have been identified in the crassulacean acid metabolism species *M. crystallinum*, the C4 plant *F. bidentis*, in poplar and in Arabidopsis (Ottow *et al.*, 2005; Cosentino *et al.*, 2010; Furumoto *et al.*, 2011). Similar to NHAD1 from *M. cyrstallinum* or *Physcomitrella patens* (Barrero-Gil *et al.*, 2007; Cosentino *et al.*, 2010), the NHD1 protein from Arabidopsis is able to complement an *E. coli* mutant lacking endogenous Na^+/H^+ transport activity (Figure 2a). The demonstration that *NHD1* expression in *E. coli* correlates with reduced endogenous sodium levels after NaCl treatment (Figure 2b) indicates that complementation is not due to activation of

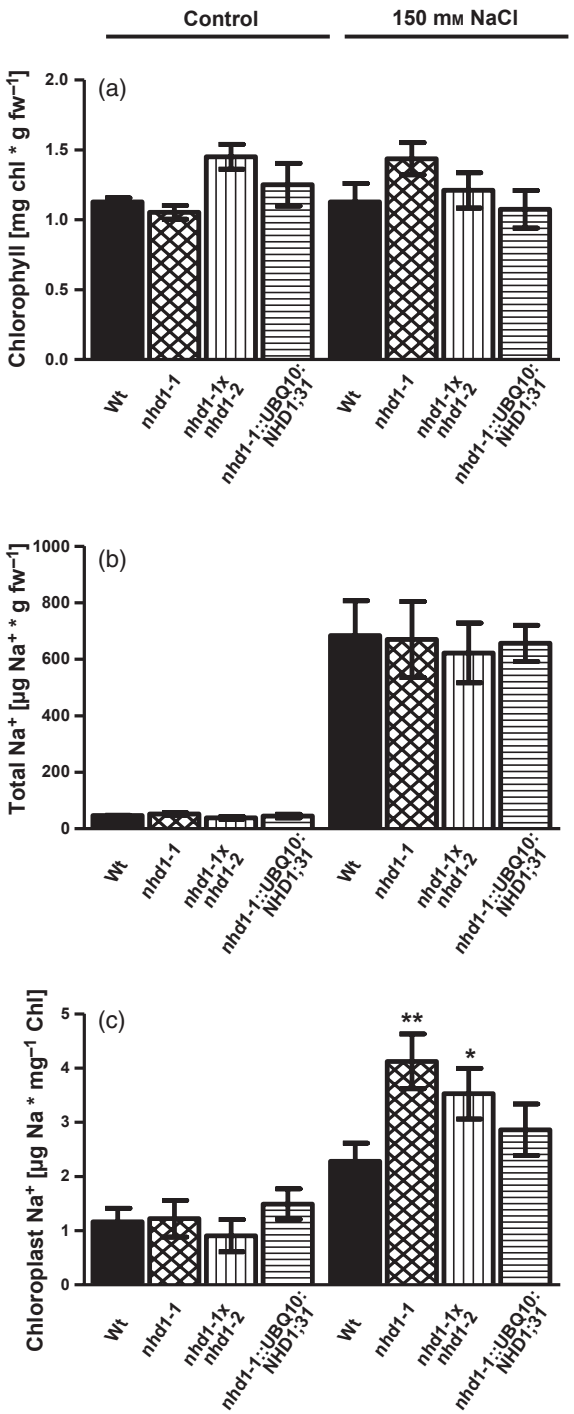

Figure 6. Sodium and chlorophyll content in Wt, *nhd1–1* and *nhd1–1::UBQ10:NHD1* plants.
Plants were watered with half-strength MS medium with or without 150 mM NaCl for 72 h prior to measurement.
(a) Chlorophyll content in leaves.
(b) Na^+ concentration in leaves, quantified by ion chromatography.
(c) Na^+ content in isolated chloroplasts, quantified by inductively coupled plasma/optical emission spectrometry.
Values are means ± SE of at least eight individual experiments. Asterisks indicate statistically significant differences compared with Wt (*$P < 0.05$, **$P < 0.01$, two-way ANOVA).

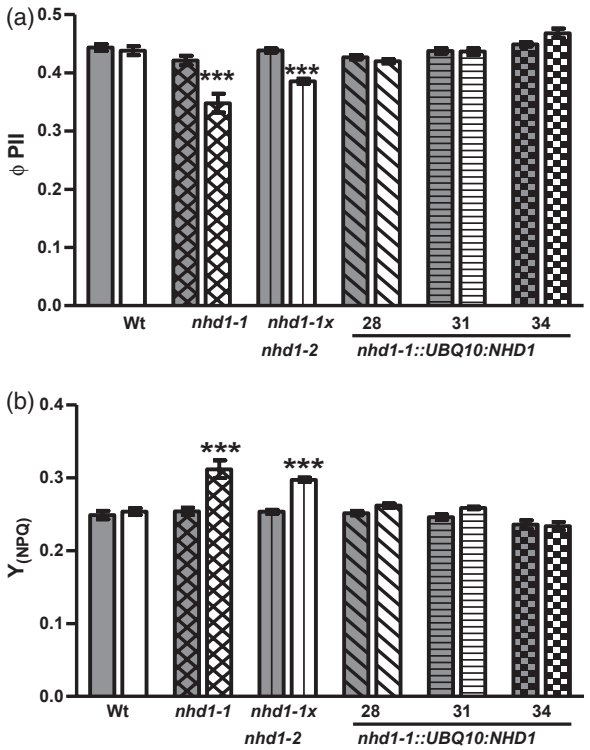

Figure 7. Effect of NaCl on photosynthetic characteristics in Wt, *nhd1–1* and *nhd1–1::UBQ10:NHD1* plants.
Plants were watered with half-strength MS medium for 4 weeks. Three days prior to measurement, 150 mM NaCl was added to the medium. Pulse-amplitude modulated analysis of ΦPII (a) and $Y_{(NPQ)}$ (b). Gray bars represent control plants, white bars represent plants watered with 150 mM NaCl for 72 h. Values are means ± SE of three individual experiments, each with three technical replicates. Asterisks indicate statistically significant differences compared with Wt (***$P < 0.001$, two-way ANOVA).

further tolerance factors or impaired movement of external sodium across the bacterial membrane.

So far, NHX1 and NHX2 are the only plant $Na^+(K^+)/H^+$ exchangers that have been purified and functionally reconstituted in proteoliposomes (Venema *et al.*, 2002; Barragan *et al.*, 2012). For these approaches, proteins were expressed heterologously in yeast (Venema *et al.*, 2002; Barragan *et al.*, 2012). As an alternative to yeast, *E. coli* cells were also successfully used for recombinant expression of various carrier proteins, including eukaryotic sodium/proton exchangers (Bibi *et al.*, 1993; Miroux and Walker, 1996; Dibrov *et al.*, 1998; Tjaden *et al.*, 1998; Uozumi *et al.*, 1998). Accordingly, we were able to express *AtNHD1* heterologously in *E. coli*, and used this recombinant protein for purification and functional reconstitution (Figure 3a–d). Thisestablished protocol helped to demonstrate genuine sodium transport in exchange with protons (Figure 3a–c). The observation that intact cells expressing *NHD1* show increased proton uptake after exposure to NaCl (Figure 3e) confirms proton/sodium exchange by the authentic protein. Moreover, the demonstration that potassium ions do not

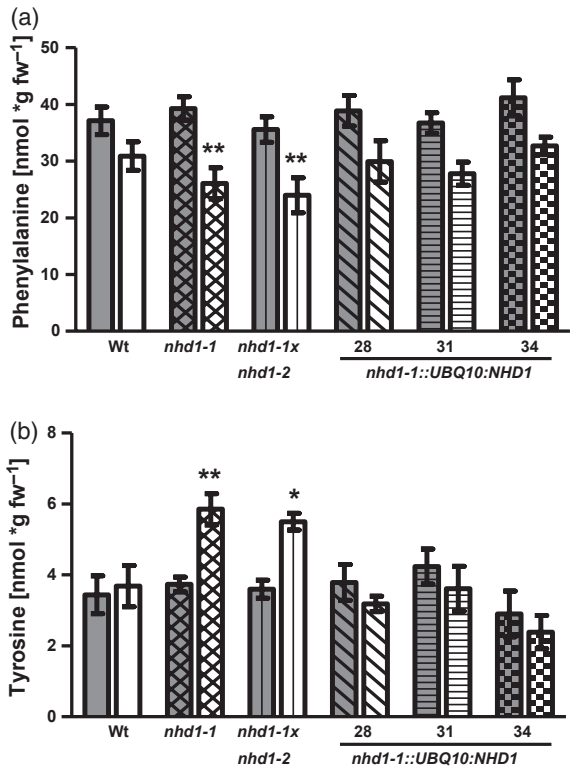

Figure 8. Effect of NaCl on phenylalanine and tyrosine levels in Wt, *nhd1–1* and *nhd1–1::UBQ10:NHD1* plants.
Plants were grown for 4 weeks on sand, and watered with or without 150 mM NaCl for three further days before phenylalanine and tyrosine levels in leaves were determined. Gray bars represent control plants (without NaCl), white bars represent samples from plants treated with NaCl. Values are means ± SE of three independent biological replicates, each with three technical replicates. Asterisks indicate statistically significant differences compared with the control (*$P < 0.05$, **$P < 0.01$, two-way ANOVA).

induce pyranine fluorescence (Figure 3d) indicates a high preference of NHD1 for sodium. In this respect, NHD1 exhibits biochemical characteristics similar to NHE1, which is located in the mammalian plasma membrane (Moncoq *et al.*, 2008). In contrast to NHD1, the endomembrane-located plant carriers NHX1 and NHX2 transport both Na^+ and K^+ after reconstitution in proteoliposomes (Venema *et al.*, 2002; Barragan *et al.*, 2012), but the potassium specificity of the plasma membrane-located salt overly sensitive 1 protein has not yet been analyzed in the reconstituted system (Quintero *et al.*, 2011).

The absence of a characteristic plastid target sequence in the poplar homolog PeNHAD1 led to the suggestion that this carrier may reside in the plasma membrane (Ottow *et al.*, 2005). In addition, NHAD1 homologs in the algae *Thalassiosira pseudonana* and *Phaeodactylum tricornutum* lack typical plastid transit peptides (Ottow *et al.*, 2005). Moreover, NHD1 from Arabidopsis was identified using a plasma membrane proteome approach (Mitra *et al.*, 2009). Together, these facts raise the possibility that at least some NHD1 proteins may locate to membranes other than the chloroplastic envelope. Thus, we performed an NHD1–GFP analysis on transformed mesophyll protoplasts from two species, namely Arabidopsis and tobacco. The distinct chloroplastic localization of the fusion protein in two independent systems (Figure 1) is in line with an *in silico* prediction of plastid localization of authentic NHD1 based on the presence of a typical N–terminally located transit peptide (Schwacke *et al.*, 2003).

Obviously, salt-adapted species tolerate extremely high stromal sodium levels, and *M. crystallinum* even promotes stromal compartmentation of sodium by increasing *McNHAD* gene expression during salt stress (Cosentino *et al.*, 2010). This reaction pattern is in strong contrast with corresponding processes in the glycophyte Arabidopsis, as non salt-stressed Wt chloroplasts contained sodium at approximately 1.2 μg Na^+ (mg Chl)$^{-1}$, and reached 2.2 μg Na^+ (mg Chl)$^{-1}$ under salt stress (Figure 6c). Assuming a stromal volume of approximately 25 μl (mg Chl)$^{-1}$ (Heldt and Sauer, 1971), the resulting sodium concentrations ranged from 0.21 mM in control chloroplasts to 0.38 mM in salt-stressed plastids. The exact cytosolic Na^+ levels under control or salt stress conditions in plants are unknown, but cytosolic sodium concentrations in a millimolar range appear reasonable under salt stress (Kronzucker and Britto, 2011). Accordingly, the glycophyte Arabidopsis keeps the stromal Na^+ level reasonably low.

Such low stromal sodium levels in *A. thaliana* (Figure 6c) are consistent with the pronounced sensitivity of photosynthetic processes in this species. Upon salt treatment, a decreased ΦPSII together with increased NPQ have been measured (Stepien and Johnson, 2009). Both of these parameters are impaired in *nhd1* knockout mutants (Figure 7a,b), which accumulate approximately twice as much sodium in the stroma compared to corresponding salt-treated wild-type plants (Figure 6c). This observation reveals that primary photosynthetic processes in chloroplasts from the glycophyte *A. thaliana* suffer at much lower sodium concentrations than present in chloroplasts from the halophytes *M. crystallinum* or *S. maritima* (Harvey *et al.*, 1981; Cosentino *et al.*, 2010). Surprisingly, enzymes from glycophytes and halophytes do not differ in their general sensitivity towards increasing sodium concentrations (Flowers *et al.*, 1977). Considering that a slight increase in stromal sodium causes significant inhibition of photosynthetic efficiency in *A. thaliana* (Figure 7a–c) (Stepien and Johnson, 2009), but probably not in halophytes, we propose that primary photosynthetic processes in these two plant groups exhibit distinct sodium sensitivity. In this respect, it is also worth mentioning that *Spinacia oleracea*, a moderately salt-sensitive species (McCue and Hanson, 1990), exhibits stromal sodium levels of approximately 28 mM after salt stress (Schroppel-Meier and Kaiser, 1988), which is between the levels of the halophytes and salt-sensitive Arabidopsis.

The observation that salt-stressed plastids from *nhd1* knockout plants exhibit increased stromal Na^+ levels compared to chloroplasts from Wt (Figure 6c) suggests that NHD1 catalyzes export of Na^+ from the stroma. This proton-coupled transport is energized during photosynthesis, as the stroma becomes alkaline (pH 8–8.5), whereas the pH in the cytosol is almost neutral (7–7.2, Werdan *et al.*, 1975). This Na^+ export is obviously efficient in Wt plants because low Na^+ levels in chloroplasts correlate with high photosynthetic activity (Figure 7), while high stromal Na^+ levels in *nhd1* mutants result in impaired photosynthesis.

We showed that a loss of NHD1 activity results in impaired photosynthesis (Figure 7a,b) and increased overall sodium sensitivity of mutants as indicated by (i) decreased fresh weight, (ii) lower chlorophyll levels, and (iii) impaired organ development (Figure 5b,d,f). We propose that the metabolic role of NHD1 is export of sodium from the chloroplast. Recently, the plastid envelope-located transporter BASS2 was identified as a sodium-coupled pyruvate co-transporter that is required for stromal synthesis of aromatic amino acids or phospho*enol*pyruvate in C4 species (Furumoto *et al.*, 2011). To maintain permanent import of pyruvate by BASS2 and to prevent toxic Na^+ levels in the chloroplast, the concomitantly imported sodium must be re-exported into the cytosol, and this has been suggested to be a function of NHD1 (Furumoto *et al.*, 2011).

Apart from sensitivity to an inhibitor (mevastatin), no phenotypes in *bass2* loss-of-function mutants were identified (Furumoto *et al.*, 2011), but, under salt stress, *nhd1* knockout mutants showed significantly decreased levels of the aromatic amino acid phenylalanine (Phe) and increased levels of tyrosine (Tyr) compared to Wt plants (Figure 8). A similar distribution of Phe and Tyr was found in the *cue1* mutant, which is deficient in the plastidic phospho*enol*pyruvate/phosphate translocator that provides the shikimate pathway with the precursor phospho*enol*pyruvate (Voll *et al.*, 2003). Similar to the situation in the *cue1* mutant, we cannot explain these reciprocal changes of Phe and Tyr content at this time. The observation that *NHD1* mRNA is highly abundant in mature Arabidopsis leaves (Figure 4a) is fully consistent with the superior importance of source leaves for net amino acid synthesis (Tegeder and Rentsch, 2010).

In summary, we conclude that Arabidopsis NHD1 functions as a chloroplast sodium exporter. The observation that loss of NHD1 activity correlates with increased stromal Na^+ levels after salt application (Figure 6c) demonstrates that NHD1 activity in Wt plants protects chloroplasts from deleterious Na^+ concentrations after salt exposure. High stromal sodium levels and hence an (at least slightly) decreased sodium gradient across the plastidial membrane might slow down pyruvate import by BASS2. Moreover, the resulting carbonic acid deficiency might affect amino acid metabolism and could explain the observed changes in aromatic amino acid levels (Figure 8). As no alteration in *NHD1* expression upon salt treatment occurs (Figure 4a), increased *NHD1* translation is required to translate low *NHD1* transcript levels (Figure 4b) into higher amounts of protein. NHD1 transport activity plays an important role in protecting vital chloroplast reactions such as photosynthesis from toxic high Na^+ levels. Consequently, highly salt-sensitive processes of primary photosynthesis are protected against harmful sodium effects.

EXPERIMENTAL PROCEDURES

Plant material and growth conditions

After stratification of *Arabidopsis thaliana* (L.) Heynh. (ecotype Columbia) seeds at 4°C for 48 h in water, seeds were sown on sand and cultivated in a growth chamber at 20°C at 125 μmol quanta m^{-2} sec^{-1} in a 10 h light/14 h dark regime conditions. Experiments were performed using 4-week-old plants watered with half-strength Murashige & Skoog (MS) medium supplemented with or without 150 mM NaCl 72 h previously. Growth in liquid culture medium was performed as described by Scheible *et al.* (2004) in half-strength MS medium. Medium was replaced after 7 days with half-strength MS medium or medium containing 100 mM NaCl.

Sequence alignment

Alignment of protein sequences was performed using CLUSTAL_X (Thompson *et al.*, 1997).

Generation of mutants

The Arabidopsis *nhd1* T–DNA insertion mutants Salk008491 (*nhd1–1*) and Sail107_F07 (*nhd1–2*) were obtained from the Arabidopsis Biological Resource Center (http://abrc.osu.edu/). An additional knockout mutant line was generated by crossing homozygous *nhd1–1* plants with pollen of heterozygous *nhd1–2* individuals. Corresponding *nhd1–1* × *nhd1–2* mutants were identified by BASTA selection and subsequent PCR. For genotyping of *nhd1* mutants, genomic DNA was isolated from 4-week-old Arabidopsis plants and used for PCR. Corresponding primers are listed in Table S2.

For complementation of the *nhd1–1* T–DNA mutant, *At3g19490* cDNA (*NHD1*) was amplified without its stop codon, and cloned into pHygII-UT-Venus-cterm (Nagai, T, Ibata, K, Park, E. S, Kubota, M, Mikoshiba, K, and Miyawaki, A., unpublished data) via the *Spe*I and *Xma*I sites. Corresponding primers are listed in Table S2. Subsequently, the plasmids were transformed into *Agrobacterium tumefaciens*. Arabidopsis transformation was performed by the floral-dip method (Clough and Bent, 1998), and positive transformants were isolated by hygromycin B selection.

Gene expression analysis

A NucleoSpin RNA plant kit (Machery-Nagel, http://www.mn-net.com/) was used to prepare total RNA from Arabidopsis plants. Any contaminating DNA was removed by DNase digestion. Quantitative RT–PCR was performed using a MyIQ cycler and IQ SYBR Green Supermix (Bio–Rad, http://www.bio-rad.com/) according to the manufacturer's instructions under the following conditions: 20 min at 50°C, 15 min at 95°C, and 50 cycles of 15 sec at 95°C, 25 sec at 58°C and 40 sec at 72°C. Relative expression levels were calculated using the $2^{-\Delta\Delta C_T}$ formula (Livak and Schmittgen, 2001), and either normalized to the value for elongation factor *EF–1α* (*At5g60390*) or to value at the onset of sodium application.

Gene-specific oligonucleotides used for quantitative RT–PCR are listed in Table S2.

Transient expression in proptplasts

Full-length *NHD1* cDNA was inserted in-frame with the GFP coding region of pGFP2 (Kost *et al.*, 1998). The primers are listed in Table S2. Purified *NHD1::pGFP2* DNA and *TAP38::pGJ1425* DNA were used to transform isolated protoplasts from *Nicotiana tabacum* cv. 38 (Wendt *et al.*, 2000) or *A. thaliana* (Yoo *et al.*, 2007). Protoplasts were analyzed using a Leica TCS SP5II confocal microscope system (http://www.leica-microsystems.com/). Scatterplot was performed using LAS AF software (Leica).

Functional complementation of an *E. coli* mutant

The *NHD1* cDNA sequence from codons 40–536 without the predicted signal peptide (ChloroP 1.1 server; http://www.cbs.dtu.dk/services/ChloroP/) was amplified by PCR and cloned in-frame into the pTAC–MAT–Tag1 vector (Sigma Aldrich, http://www.sigmaaldrich.com/). Primers are listed in Table S2. Functional complementation of the *E. coli* knockout strain *KNabc* (Δ*nha*A::Km^r, Δ*nha*B::Em^r, Δ*cha*A::Cm^r, Nozaki *et al.*, 1996) was performed as described by Ottow *et al.* (2005). *KNabc* cells were either transformed with *NHD1::pTAC-MAT-Tag1* or with empty pTAC-MAT-Tag1 vector as a control. Cells were grown in LBK medium [1% tryptone, 0.5% yeast extract and 1% KCl (pH 7.5)]. Bacterial growth was analyzed by fitting the data to the Boltzman equation:

$$y = \frac{OD_0 - OD_{max}}{1 + (t/t_{1/2})^p} + OD_{max}$$

where OD_0 and OD_{max} correspond to the initial and final optical density. The time when half of OD_{max} was reached is indicated by $t_{1/2}$, and p indicates the growth exponent.

Bacterial element analyses

Element analyses in *KNabc* cells were performed as described by Ottow *et al.* (2005). Bacteria were centrifuged (5000 ***g***, 10 min, 4°C) and washed twice (5000 ***g***, 10 min, 4°C) in potassium phosphate buffer medium (170 mM KH_2PO_4, 720 mM K_2HPO_4). Samples were lyophilized for 48 h prior to sodium measurement by inductively coupled plasma/optical emission spectrometry.

pH-dependent sodium transport measurement

isopropyl-β–D–thiogalactopyranoside-induced *KNabc* cells were adjusted to an OD_{600} of 7 using 0.5 mM HEPES buffer (pH 7.0). Either 0 or 500 mM NaCl was added, and the cells were pelleted immediately (5000 ***g***, 5 min, 4°C). Proton-coupled sodium transport was measured as an increase in pH in the supernatant.

Recombinant protein expression and IMAC purification of NHD1

Recombinant protein synthesis and IMAC purification was performed exactly as described by Trentmann *et al.* (2007).

SDS–PAGE and immunostaining

Prior to separation by SDS-PAGE proteins were mixed with 6 × concentrated sample buffer medium (375 mM Tris/HCl, pH 6.8, 0.3% SDS, 60% glycerol, 1.5% bromophenol blue). Electrophoretic protein separation was performed in a discontinuous, denaturing system with a 3% stacking and a 12% separating polyacrylamide gels as described by Laemmli (1970). Afterwards, proteins were visualized in the gel by staining with Coomassie Brilliant Blue R250 or transferred to a nitrocellulose membrane in a wet-blotting apparatus. Immunodetection was performed using a monoclonal mouse anti poly His IgG (Sigma) in combination with a secondary horseradish anti-mouse IgG (Sigma). The molecular masses were estimated using a Page Ruler™ pre-stained protein ladder (Thermo Scientific, http://www.thermoscientific.com/).

Reconstitution and activity measurement of NHD1

Reconstitution of NHD1 into proteoliposomes and activity measurement were performed as described by Moncoq *et al.* (2008) with minor changes. *E. coli* total lipid extract (Avanti, http://avantilipids.com/) was dried to a thin film under nitrogen gas, and lyophilized. Dried lipids were mixed with reconstitution buffer (20 mM bis-tris propane/MES, pH 7.5, 50 mM NH_4Cl) supplemented with 2.5 mM of the fluorescent pH indicator pyranine, and vortexed (30 s, max. speed). *n*–octyl-D–glucoside (20%) was added, and the mixture was vortexed (30 s, max. speed) until all lipid was solubilized. Purified NHD1 was added and mixed gently. The solubilized protein/lipid/detergent mixture was applied to a 2 ml Sephadex G–50 column (GE Healthcare, http://www3.gehealthcare.de/) pre-loaded with reconstitution buffer containing pyranine. The column eluate was incubated for 30 min at room temperature with SM–2 Bio-Beads (BIO-RAD, http://www.bio-rad.com/) to remove residual detergent. The sample was applied to a 2 ml Sephadex G–50 column equilibrated with reconstitution buffer without pyranine. The resultant proteoliposomes containing NHD1 were monitored for $Na^+(K^+)/H^+$ exchange activity via pyranine fluorescence using a spectrofluorometer, at an excitation wavelength of 463 nm and an emission wavelength of 510 nm. Proteoliposomes containing NHD1 and control proteoliposomes reconstituted in the same way using SERCA (purified from rabbit skeletal muscle as described by Stokes and Green, 1990) were added to a 2 ml reaction cuvette containing ammonium-free reaction buffer (20 mM bis-tris propane/MES, pH 7.5) to generate a pH gradient. NaCl or KCl was added to initiate $Na^+(K^+)/H^+$ exchange, which was monitored by the increase in pyranine fluorescence.

Isolation of intact chloroplasts

Isolation of chloroplasts was performed as described by Aronsson and Jarvis (2011) with some modifications. Leaves of 4-week-old plants were harvested in the dark, homogenized five times in isolation buffer medium (0.3 M sorbitol, 5 mM $MgCl_2$, 5 mM EGTA, 5 mM EDTA, 10 mM $KHCO_3$, 20 mM HEPES, pH 8.0), and filtered through a double layer of Miracloth (Calbiochem, http://www.merckmillipore.com/). After centrifugation (1000 ***g***, 5 min, 4°C), the pellet was resuspended in isolation buffer medium, transferred to a linear Percoll (GE Healthcare) gradient [50% isolation buffer medium, 50% Percoll, 10 mg glutathione, pre-spun (43 000 ***g***, 30 min, 4°C)] and centrifuged (7800 ***g***, 10 min, 4°C). Intact chloroplasts were harvested from the lower green band of the gradient, washed with HMS buffer [0.3 M sorbitol, 3 mM $MgSO_4$, 50 mM HEPES, pH 8.0 and pelleted (600 ***g***, 5 min, 4°C)]. The intactness and purity of isolated chloroplasts was confirmed by measuring marker enzymes (phosphoglucoisomerase for intactness, NADP-GAPDH for chloroplasts, UDP-glucose pyrophosphorylase for cytosol, and fumerase for mitochondria) in isolated chloroplasts and whole-leaf extracts. Purified chloroplasts displayed an intactness of 91 ± 1.3%, cytosolic contamination of 1.6 ± 0.4%, and mitochondrial contamination of 3.2 ± 0.7%.

Chlorophyll determination

The chlorophyll content of isolated chloroplasts and leaves was quantified as described by Arnon (1949).

Sodium quantification

Prior to sodium quantification, chloroplasts were digested using a temperature step gradient with a maximum temperature of 210°C in a MLS-Ethos microwave (http://www.mls-mikrowellen.de/) oven with 5 ml HNO_3 (60% v/v), 2 ml H_2O_2 (30% v/v), and diluted to a final volume of 12 ml with double-distilled water. Analysis was performed by inductively coupled plasma/optical emission spectrometry on an iCAP 6300 DUO apparatus (http://www.mls-mikrowellen.de/). Sodium was detected and quantified at 589.5 nm. For sodium quantification in rosettes, leaves were ground in liquid nitrogen, resuspended in double-distilled water and centrifuged. Ion contents of the extracts were analyzed by a 761–IC compact system (Metrohm, http://metrohm.de/), equipped with a Metrosep-C4-150 column (Metrohm).

Pulse-amplitude modulated fluorometry

Chlorophyll fluorescence was measured using a MINI Imaging pulse-amplitude modulation fluorometer (Walz, http://www.walz.com/). Prior to measurement, 4-week-old plants were adapted to the dark for 5 min. The quantum yield of photochemical energy conversion on PSII (Φ_{PSII}) and the quantum yield of non-photochemical quenching of chlorophyll fluorescence $Y_{(NPQ)}$ were determined.

Amino acid quantification

To determine the amount of free amino acids, leaves were ground in liquid nitrogen, and extracted with 80% ethanol at 80°C for 1 h. The supernatant was evaporated to dryness in a vacuum centrifuge. The amino acids and standards (20 mM each) were derivatized as described previously (Rolletschek *et al.*, 2002) using 6-aminoquinolyl-carbamyl (AQC) (Watrex, http://www.watrex.com/). Measurements of the AQC amino acids were performed using a Dionex P680 HPLC system with an UV170U detector (Dionex, http://www.dionex.com/), and a column system consisting of a CC8/4 ND 100–5 C18–ec column and a 250/4 Nucledur 100–5 C18–ec column (Macherey-Nagel). A gradient comprising 100 mM sodium acetate and acetonitrile (0–15%) was used to separate the amino acids. The AQC amino acids were detected by fluorescence with excitation at 250 nm and emission at 395 nm.

ACKNOWLEDGEMENTS

We thank Dario Leister and Mathias Pribil (Plant Molecular Biology, Ludwig Maximilians University, Munich, Germany) for providing the *TAP38::pGJ1425* DNA construct. Work in the laboratories of H.E.N. was financially supported by the Deutsche Forschungsgemeinschaft (IRTG 1830). Work in the laboratories of H.E.N. was further supported by the Landesschwerpunkt 'Membrantransport' (http://www.uni-kl.de/rimb). This work was also supported by the Human Frontier Science Program, the Alexander von Humboldt Foundation (to H.–H.K.) and the US National Science Foundation (MCB0918220). Isolation of mutants, fusion proteins and complementation lines was supported by a grant from the Division of Chemical Sciences, Geosciences and Biosciences, Office of Basic Energy Sciences, US Department of Energy (DE-FG02-03ER15449) (to J.I.S.).

SUPPORTING INFORMATION

Additional Supporting Information may be found in the online version of this article.

Figure S1. Alignment of the amino acid sequence from AtNHD1 with that of its homolog NHAD from *M. crystallinum*.

Figure S2. Subcellular localization of NHD1–GFP and TAP38–RFP fusion proteins.

Figure S3. Growth of the *E. coli* knockout strain *KNabc* after transformation with empty pTAC-MAT-Tag1 vector or *NHD1::pTAC-MAT-Tag1*.

Figure S4. Characterization of *nhd1* mutant plants.

Table S1. Amino acid quantification in non-stressed and salt-stressed Wt, *nhd1* knockout and *nhd1–1::UBQ10:NHD1* plants.

Table S2. Oligonucleotides used for genotyping of *nhd1* T–DNA insertion lines, complementation of *nhd1–1* with *AtNHD1* and quantitative RT–PCR analysis.

REFERENCES

Apse, MP, Aharon, GS, Snedden, WA and Blumwald, E (1999) Salt tolerance conferred by overexpression of a vacuolar Na^+/H^+ antiport in Arabidopsis. *Science*, **285**, 1256–1258.

Arnon, DI (1949) Copper enzymes in isolated chloroplasts. Polyphenol oxidase in *Beta vulgaris*. *Plant Physiol.* **24**, 1–4.

Aronsson, H and Jarvis, RP (2011) Rapid isolation of Arabidopsis chloroplasts and their use for *in vitro* protein import assays. *Methods Mol. Biol.* **774**, 281.

Barragan, V, Leidi, EO, Andres, Z, Rubio, L, De Luca, A, Fernandez, JA, Cubero, B and Pardo, JM (2012) Ion exchangers NHX1 and NHX2 mediate active potassium uptake into vacuoles to regulate cell turgor and stomatal function in Arabidopsis. *Plant Cell*, **24**, 1127–1142.

Barrero-Gil, J, Rodriguez-Navarro, A and Benito, B (2007) Cloning of the PpNHAD1 transporter of *Physcomitrella patens*, a chloroplast transporter highly conserved in photosynthetic eukaryotic organisms. *J. Exp. Bot.* **58**, 2839–2849.

Bartels, D and Sunkar, R (2005) Drought and salt tolerance in plants. *Crit. Rev. Plant Sci.* **24**, 23–58.

Bassil, E, Ohto, M, Esumi, T, Tajima, H, Zhu, Z, Cagnac, O, Belmonte, M, Peleg, Z, Yamaguchi, T and Blumwald, E (2011) The Arabidopsis intracellular Na^+/H^+ antiporters NHX5 and NHX6 are endosome associated and necessary for plant growth and development. *Plant Cell*, **23**, 224–239.

Bibi, E, Gros, P and Kaback, HR (1993) Functional expression of mouse *mdr1* in *Escherichia coli*. *Proc. Natl Acad. Sci. USA*, **90**, 9209–9213.

Blumwald, E (2000) Sodium transport and salt tolerance in plants. *Curr. Opin. Cell Biol.* **12**, 431–434.

Brett, CL, Donowitz, M and Rao, R (2005) Evolutionary origins of eukaryotic sodium/proton exchangers. *Am. J. Physiol. Cell Physiol.* **288**, C223–C239.

Chen, H and Fliegel, L (2008) Expression, purification, and reconstitution of the Na^+/H^+ exchanger *sod2* in *Saccharomyces cerevisiae*. *Mol. Cell. Biochem.* **319**, 79–86.

Clough, SJ and Bent, AF (1998) Floral dip: a simplified method for *Agrobacterium*-mediated transformation of *Arabidopsis thaliana*. *Plant J.* **16**, 735–743.

Cosentino, C, Fischer-Schliebs, E, Bertl, A, Thiel, G and Homann, U (2010) Na^+/H^+ antiporters are differentially regulated in response to NaCl stress in leaves and roots of *Mesembryanthemum crystallinum*. *New Phytol.* **186**, 669–680.

Dibrov, P, Young, PG and Fliegel, L (1998) Physiological consequences of expression of the Na^+/H^+ antiporter SOD2 in *Escherichia coli*. *Mol. Cell. Biochem.* **183**, 125–132.

Flowers, TJ and Colmer, TD (2008) Salinity tolerance in halophytes. *New Phytol.* **179**, 945–963.

Flowers, TJ and Dalmond, D (1992) Protein synthesis in halophytes: the influence of potassium, sodium and magnesium *in vitro*. *Plant Soil*, **146**, 153–161.

Flowers, TJ, Troke, PF and Yeo, AR (1977) The mechanism of salt tolerance in halophytes. *Annu. Rev. Plant. Physiol.* **28**, 89–121.

Furumoto, T, Yamaguchi, T, Ohshima-Ichie, Y *et al.* (2011) A plastidial sodium-dependent pyruvate transporter. *Nature*, **476**, 472–475.

Harvey, DMR, Hall, JL, Flowers, TJ and Kent, B (1981) Quantitative ion localization within *Suaeda maritima* leaf mesophyll cells. *Planta*, **151**, 555–560.

Heldt, HW and Sauer, F (1971) The inner membrane of the chloroplast envelope as the site of specific metabolite transport. *Biochim. Biophys. Acta*, **234**, 83–91.

Hernandez, A, Jiang, X, Cubero, B, Nieto, PM, Bressan, RA, Hasegawa, PM and Pardo, JM (2009) Mutants of the *Arabidopsis thaliana* cation/H^+ antiporter AtNHX1 conferring increased salt tolerance in yeast: the endosome/prevacuolar compartment is a target for salt toxicity. *J. Biol. Chem.* **284**, 14276–14285.

Horie, T, Hauser, F and Schroeder, JI (2009) HKT transporter-mediated salinity resistance mechanisms in Arabidopsis and monocot crop plants. *Trends Plant Sci.* **14**, 660–668.

Kost, B, Spielhofer, P and Chua, NH (1998) A GFP–mouse talin fusion protein labels plant actin filaments *in vivo* and visualizes the actin cytoskeleton in growing pollen tubes. *Plant J.* **16**, 393–401.

Krebs, M, Held, K, Binder, A, Hashimoto, K, Den Herder, G, Parniske, M, Kudla, J and Schumacher, K (2012) FRET-based genetically encoded sensors allow high-resolution live cell imaging of Ca^{2+} dynamics. *Plant J.* **69**, 181–192.

Kronzucker, HJ and Britto, DT (2011) Sodium transport in plants: a critical review. *New Phytol.* **189**, 54–81.

Laemmli, UK (1970) Cleavage of structural proteins during the assembly of the head of bacteriophage T4. *Nature*, **227**, 680–685.

Livak, JK and Schmittgen, TD (2001) Analysis of relative gene expression data using real-time quantitative PCR and the $2^{-\Delta\Delta C_T}$ method. *Methods*, **25**, 402–408.

Martinoia, E, Maeshima, M and Neuhaus, HE (2007) Vacuolar transporters and their essential role in plant metabolism. *J. Exp. Bot.* **58**, 83–102.

Mäser, P, Eckelman, B, Vaidyanathan, R *et al.* (2002) Altered shoot/root Na^+ distribution and bifurcating salt sensitivity in Arabidopsis by genetic disruption of the Na^+ transporter AtHKT1. *FEBS Lett.* **531**, 157–161.

Maxwell, K and Johnson, GN (2000) Chlorophyll fluorescence – a practical guide. *J. Exp. Bot.* **51**, 659–668.

McCue, KF and Hanson, AD (1990) Drought and salt tolerance: towards understanding and application. *Trends Biotechnol.* **8**, 358–362.

Miroux, B and Walker, JE (1996) Over-production of proteins in *Escherichia coli*: mutant hosts that allow synthesis of some membrane proteins and globular proteins at high levels. *J. Mol. Biol.* **260**, 289–298.

Mitra, SK, Walters, BT, Clouse, SD and Goshe, MB (2009) An efficient organic solvent based extraction method for the proteomic analysis of Arabidopsis plasma membranes. *J. Proteome Res.* **8**, 2752–2767.

Moncoq, K, Kemp, G, Li, X, Fliegel, L and Young, HS (2008) Dimeric structure of human Na^+/H^+ exchanger isoform 1 overproduced in *Saccharomyces cerevisiae*. *J. Biol. Chem.* **283**, 4145–4154.

Munns, R (2005) Genes and salt tolerance: bringing them together. *New Phytol.* **167**, 645–663.

Nozaki, K, Inaba, K, Kuroda, T, Tsuda, M and Tsuchiya, T (1996) Cloning and sequencing of the gene for Na^+/H^+ antiporter of *Vibrio parahaemolyticus*. *Biochem. Biophys. Res. Commun.* **222**, 774–779.

Ohta, M, Hayashi, Y, Nakashima, A, Hamada, A, Tanaka, A, Nakamura, T and Hayakawa, T (2002) Introduction of a Na^+/H^+ antiporter gene from *Atriplex gmelini* confers salt tolerance to rice. *FEBS Lett.* **532**, 279–282.

Ottow, EA, Polle, A, Brosche, M, Kangasjarvi, J, Dibrov, P, Zorb, C and Teichmann, T (2005) Molecular characterization of PeNhaD1: the first member of the NhaD Na^+/H^+ antiporter family of plant origin. *Plant Mol. Biol.* **58**, 75–88.

Pavon, LR, Lundh, F, Lundin, B, Mishra, A, Persson, BL and Spetea, C (2008) Arabidopsis ANTR1 is a thylakoid Na^+-dependent phosphate transporter: functional characterization in *Escherichia coli*. *J. Biol. Chem.* **283**, 13520–13527.

Pribil, M, Pesaresi, P, Hertle, A, Barbato, R and Leister, D (2010) Role of plastid protein phosphatase TAP38 in LHC II dephosphorylation and thylakoid electron flow. *PLoS Biol.* **8**, e1000288.

Quintero, FJ, Martinez-Atienza, J, Villalta, I *et al.* (2011) Activation of the plasma membrane Na/H^+ antiporter Salt-Overly-Sensitive 1 (SOS1) by phosphorylation of an auto-inhibitory C–terminal domain. *Proc. Natl Acad. Sci. USA*, **108**, 2611–2616.

Rolletschek, H, Hajirezaei, M-R, Wobus, U and Weber, H (2002) Antisense inhibition of ADP-glucose pyrophosphorylase in *Vicia narbonensis* seeds increases soluble sugars and leads to higher water and nitrogen uptake. *Planta*, **214**, 954–964.

Scheible, WR, Morcuende, R, Czechowski, T, Fritz, C, Osuna, D, Palacios-Rojas, N, Schindelasch, D, Thimm, O, Udvardi, MK and Stitt, M (2004) Genome-wide reprogramming of primary and secondary metabolism, protein synthesis, cellular growth processes, and the regulatory infrastructure of Arabidopsis in response to nitrogen. *Plant Physiol.* **136**, 2483–2499.

Schroppel-Meier, G and Kaiser, WM (1988) Ion homeostasis in chloroplasts under salinity and mineral deficiency: I. Solute concentrations in leaves and chloroplasts from spinach plants under NaCl or $NaNO_3$ salinity. *Plant Physiol.* **87**, 822–827.

Schwacke, R, Schneider, A, van der Graf, E, Fischer, K, Catoni, E, Desimone, M, Frommer, WB, Flügge, UI and Kunze, R (2003) ARAMEMNON, a novel database for Arabidopsis integral membrane proteins. *Plant Physiol.* **131**, 16–26.

Stepien, P and Johnson, GN (2009) Contrasting responses of photosynthesis to salt stress in the glycophyte Arabidopsis and the halophyte Thellungiella: role of the plastid terminal oxidase as an alternative electron sink. *Plant Physiol.* **149**, 1154–1165.

Stokes, DL and Green, NM (1990) Three-dimensional crystals of CaATPase from sarcoplasmic reticulum. Symmetry and molecular packing. *Biophys. J.* **57**, 1–14.

Tegeder, M and Rentsch, D (2010) Uptake and partitioning of amino acids and peptides. *Mol. Plant*, **3**, 997–1011.

Thompson, JD, Gibson, TJ, Plewniak, F, Jeanmougin, F and Higgins, DG (1997) The CLUSTAL_X windows interface: flexible strategies for multiple sequence alignment aided by quality analysis tools. *Nucleic Acids Res.* **25**, 4876–4882.

Tjaden, J, Schwöppe, C, Möhlmann, T and Neuhaus, HE (1998) Expression of the plastidic ATP/ADP transporter gene in *Escherichia coli* leads to a functional adenine nucleotide transport system in the bacterial cytoplasmic membrane. *J. Biol. Chem.* **273**, 9630–9636.

Trentmann, O, Horn, M, Terwisscha van Scheltinga, AC, Neuhaus, HE and Haferkamp, I (2007) Enlightening energy parasitism by analysis of an ATP/ADP transporter from Chlamydiae. *PLoS Biol.* **5**, e231.

Uozumi, N, Nakamura, T, Schroeder, JI and Muto, S (1998) Determination of transmembrane topology of an inward-rectifying potassium channel from *Arabidopsis thaliana* based on functional expression in *Escherichia coli*. *Proc. Natl Acad. Sci. USA*, **95**, 9773–9778.

Venema, K, Quintero, FJ, Pardo, JM and Donaire, JP (2002) The Arabidopsis Na^+/H^+ exchanger AtNHX1 catalyzes low affinity Na^+ and K^+ transport in reconstituted liposomes. *J. Biol. Chem.* **277**, 2413–2418.

Voll, L, Häusler, RE, Hecker, R, Weber, A, Weissenböck, G, Fiene, G, Waffen, S and Flügge, UI (2003) The phenotype of the Arabidopsis *cue1* mutant is not simply caused by a general restriction of the shikimate pathway. *Plant J.* **36**, 301–317.

Wendt, UK, Wenderoth, I, Tegeler, A and Von Schaewen, A (2000) Molecular characterization of a novel glucose-6-phosphate dehydrogenase from potato (*Solanum tuberosum* L.). *Plant J.* **23**, 723–733.

Werdan, K, Heldt, HW and Milovancev, M (1975) The role of pH in the regulation of carbon fixation in the chloroplast stroma. Studies on CO_2 fixation in the light and dark. *Biochim. Biophys. Acta*, **396**, 276–292.

Xue, ZY, Zhi, DY, Xue, GP, Zhang, H, Zhao, YX and Xia, GM (2004) Enhanced salt tolerance of transgenic wheat (*Triticum aestivum* L.) expressing a vacuolar Na^+/H^+ antiporter gene with improved grain yields in saline soils in the field and a reduced level of leaf Na^+. *Plant Sci.* **167**, 849–859.

Yin, XY, Yang, AF, Zhang, KW and Zhang, JR (2004) Production and analysisof transgenic maize with improved salt tolerance by the introduction of AtNHX1 gene. *Acta Bot. Sin.* **7**, 12–20.

Yokoi, S, Quintero, FJ, Cubero, B, Ruiz, MT, Bressan, RA, Hasegawa, PM and Pardo, JM (2002) Differential expression and function of *Arabidopsis thaliana* NHX Na^+/H^+ antiporters in the salt stress response. *Plant J.* **30**, 529–539.

Yoo, SD, Cho, YH and Sheen, J (2007) Arabidopsis mesophyll protoplasts: a versatile cell system for transient gene expression analysis. *Nat. Protoc.* **2**, 1565–1572.

Zhang, H-X and Blumwald, E (2001) Transgenic salt-tolerant tomato plants accumulate salt in foliage but not in fruit. *Nat. Biotechnol.* **19**, 765–768.

Zhang, H-X, Hodson, JN, Williams, JP and Blumwald, E (2001) Engineering salt-tolerant *Brassica* plants: characterization of yield and seed oil quality in transgenic plants with increased vacuolar sodium accumulation. *Proc. Natl Acad. Sci. USA*, **98**, 12832–12836.

Zhu, JK (2002) Salt and drought stress signal transduction in plants. *Annu. Rev. Cell Biol.* **53**, 247–273.